

Document downloaded from:

<http://hdl.handle.net/10251/165905>

This paper must be cited as:

Lujan Facundo, MJ.; Iborra-Clar, MI.; Mendoza Roca, JA.; Alcaina-Miranda, MI.; Maciá, AM.; Lardin, C.; Pastor, L.... (2020). Preparation of Sewage Sludge-Based Activated Carbon for Hydrogen Sulphide Removal. *Water Air & Soil Pollution*. 231(4):1-12.  
<https://doi.org/10.1007/s11270-020-04518-w>



The final publication is available at

<https://doi.org/10.1007/s11270-020-04518-w>

Copyright Springer-Verlag

Additional Information

1 **Preparation of sewage sludge-based activated carbon for hydrogen sulfide removal**

2  
3 M.J. Luján-Facundo<sup>1</sup>, M.I. Iborra-Clar<sup>1</sup>, J.A. Mendoza-Roca<sup>1</sup>, M.I. Alcaina-  
4 Miranda<sup>1</sup>, A.M. Maciá<sup>2</sup>, C. Lardín<sup>3</sup>, L. Pastor<sup>4</sup>, J. Claros<sup>4</sup>.

5  
6 Corresponding author: M.J. Luján-Facundo<sup>1</sup>, [malufa@etsii.upv.es](mailto:malufa@etsii.upv.es)

7  
8 <sup>1</sup>Instituto de Seguridad Industrial, Radiofísica y Medioambiental, Universitat Politècnica  
9 de València, Camino de Vera, s/n, Valencia 46022 (Spain).

10 <sup>2</sup>Molina del Segura WWTP. UTE Molina del Segura – Alguazas. Address: Campotéjar  
11 Baja, s/n bajo, 30500 Molina del Segura, Murcia, Spain.

12 <sup>3</sup>Regional Entity for Sanitation and Wastewater Treatment in Murcia, Spain  
13 (ESAMUR). Address: Complejo Espinardo CN-301, Calle Santiago Navarro, 4, 30100  
14 Espinardo, Murcia.

15 <sup>4</sup>Depuración de Aguas del Mediterráneo (DAM). Avenida Benjamín Franklin, 21.  
16 46980 Parque Tecnológico, Paterna, Valencia (Spain).

17  
18  
19 **Keywords:** activated carbon, adsorption, deodorization, wastewater sludge.

## 23 **Abstract**

24 The circular economy concept boosts the use of wastes as secondary raw materials in  
25 the EU renewable and sustainable framework. In wastewater treatment plants (WWTP)  
26 sludge is one of the most important waste and its management is being widely discussed  
27 in the last years. In this work, sewage sludge from WWTP was employed as raw  
28 material for producing activated carbon (AC) by physical-chemical activation. The  
29 prepared AC was subsequently tested for hydrogen sulfide removal in view of its further  
30 use in deodorization in a WWTP. The effects of the activation temperature and the  
31 chemical agent used (NaOH and KOH) during the activation process were studied. On  
32 the one hand, the characteristics of each AC fabricated were analyzed in terms of BET  
33 (Brunauer-Emmett-Teller) surface area, pore and micropore volume, pore diameter,  
34 surface morphology and zeta potential. On the other hand, BET isotherms were also  
35 calculated. Finally, both the prepared AC and a commercial AC were tested for H<sub>2</sub>S  
36 removal from a gas stream. Results demonstrated that the optimum physical and  
37 chemical activation temperature was 600°C and 1000°C, respectively and the best  
38 activated agent tested was KOH. The prepared AC showed excellent properties (specific  
39 surface area around 300 m<sup>2</sup>/g) for H<sub>2</sub>S removal, even better efficiencies than those  
40 achieved by the tested commercial AC.

41

42

## 43 **1. Introduction**

44 In the last years the emerging concept of circular economy is changing the mission of  
45 wastewater treatment plants. The main goal of these plants is no longer to discharge the  
46 treated effluent meeting the legal standards but to recover energy and materials from the

47 wastewater. In this way, nutrients recovery(Peng et al. 2018; Ye et al. 2018),  
48 optimization of energy recovery from anaerobic processes(Kimura et al. 2017)and  
49 sludge valorization are topics of increasing interest.

50 Sludge management is a non-solved issue. The reuse of wastewater sludge for  
51 agricultural purposes is threatened by the presence of persistent organic compounds and  
52 pathogens and some countries have restricted the use of wastewater sludge in the  
53 agriculture(G. Mininni et al. 2015).

54 One of the applications studied for the wastewater sludge in recent years has been its  
55 use for making activated carbon. The interest for the preparation of activated carbon  
56 from organic wastes increased in the last decade of the 20<sup>th</sup> century as reported by Dias  
57 et al.(2007). These authors summarized the wastes used for the activated carbon  
58 preparation and the applications of the prepared carbons. In this way, cherry stones,  
59 corn cobs, olive pits, walnut shells and other wastes have been employed for this  
60 purpose.Chiavola (2013)reviewed the main findings about the valorization of organic  
61 wastes as activated carbon. This author summarizes the use of activated carbon prepared  
62 from peanut shells, olive stone and apricot stone of different works.

63 The aforementioned trend to circular economy implies that valorization of organic  
64 wastes as activated carbon is still a current goal especially when high amounts of  
65 organic wastes are available. As an example, Pandiarajan et al.(2018) prepared activated  
66 carbon from orange peel to separate herbicides. Activation was carried out using KOH  
67 in the ratio 1:2 and reaching temperatures of 700°C.Other examples are works in which  
68 authors have used coconut(Andrade et al. 2018)and corncob(Zhu et al. 2018).

69 Focusing on wastewater sludge, it has to be highlighted that sludge is theoretically an  
70 appropriate source for activated carbon due to great availability and high organic matter

71 content. Li et al. (2011) and Wang et al. (2008) prepared activated carbon from activated  
72 sludge from a municipal wastewater treatment plant and from sludge from a paper mill  
73 wastewater treatment plant, respectively. In both cases the prepared activated carbon  
74 was used for dyes removal. More recently, Qiu and Huang (2015) made activated carbon  
75 from sewage sludge using  $ZnCl_2$  for the activation with the aim of separating two  
76 commercial dyes from wastewater. Other applications of sludge-based activated carbons  
77 are the separation of heavy metals (Li et al. 2018) and pharmaceutical compounds (dos  
78 Reis et al. 2016).

79 Concerning the preparation processes, Hadi et al. (2015) concluded in a review article  
80 that chemical activation yielded considerable higher specific surface areas than physical  
81 activation procedures. In this way, it is very important to focus on chemical activation.

82 In this work, chemically activated carbon from sewage sludge has been prepared for  
83 hydrogen sulfide adsorption. Until now, there are limited papers dealing with this topic.  
84 Only Li et al. (2015) aimed at this application. However, it would be of great  
85 importance to use the sludge in the same wastewater treatment plant for odour  
86 elimination, for example in the final step of thickeners or in the sludge dehydration. In  
87 addition, preparation of the activated carbon in the same plant would avoid transport  
88 costs. This fact together with the uncertainty about the future sludge management  
89 alternatives make that the preparation of activated carbon for hydrogen sulfide removal  
90 may have a promising future.

91

92

93

94 **2. Materials and methods**

95

96 2.1. Sludge characterization

97 Sludge from municipal WWTP located in Murcia Region (Spain) was used for activated  
98 carbon preparation. The characterization of the sludge included the measurement of  
99 pH, conductivity, total suspended solids (TSS), volatile suspended solids (VSS),  
100 total COD (chemical oxygen demand) and ammonium nitrogen ( $\text{NH}_4\text{-N}$ ). In addition,  
101 sludge was also pre-treated in order to measure the following parameters in the soluble  
102 fraction: soluble COD, total nitrogen (TN), nitrates ( $\text{NO}_3\text{-N}$ ), total phosphorous (TP),  
103 calcium ( $\text{Ca}^{+2}$ ) and magnesium ( $\text{Mg}^{+2}$ ). The pre-treatment consisted in centrifuging at  
104 10.000 rpm for 15 min and filtering the clarified water for the analysis.

105 pH and conductivity measurements were carried out with pH Meter GLP 21<sup>+</sup> and EC-  
106 Meter GLP 31<sup>+</sup> (CRISON), respectively. TSS and VSS were measured according to  
107 Standard Methods (APHA, AWWA, WEF, 2005). COD, TN,  $\text{NO}_3\text{-N}$ , TP,  $\text{Ca}^{+2}$  and  
108  $\text{Mg}^{+2}$  were analyzed using kits from Merck (Spain).  $\text{NH}_4\text{-N}$  content was determined  
109 using a “Pro-Nitro M” distiller (P-Selecta, Spain).

110 The properties of the analyzed sludge are in Table 1. It can be observed that all the  
111 parameters are in the range for sludge characterization (Ping et al., 2020). In addition,  
112 the high COD content is especially favourable for activated carbon preparation (Li et al.  
113 2020).

114

115

116

**Table 1: Sludge characterization for activated carbon preparation.**

<b>Parameter</b>	<b>Value</b>
TN (mg/L)	1370
NO <sub>3</sub> -N (mg/L)	8.84
PT (mg/L)	51.30
Total COD (mg/L)	7683
Soluble COD (mg/L)	1569
Ca <sup>+2</sup> (mg/L)	180.30
Mg <sup>+2</sup> (mg/L)	60
NH <sub>4</sub> -N (mg/L)	949.45
pH	7.80
Conductivity (mS/cm)	16.71
TSS (g/L)	7.55
VSS (g/L)	4

117

118

## 119 2.2. Activated carbon preparation

120 Two series of experiments were performed in the AC preparation. In the first one,  
121 NaOH and KOH (from Panreac) were used as activating agents. Table 2 summarizes the  
122 experimental values of the variables used during the first set of experiments. The  
123 physical activation is a pyrolysis process and the chemical activation was carried out by  
124 mixing the sludge with the activated agent. The heat treatment of the samples was  
125 conducted in a furnace from Nabertherm model RSRB 120/750/11. Pure nitrogen gas  
126 was used to produce an inert gas atmosphere. The flow rate of nitrogen was 300  
127 ml/min and samples were heated up to the previously programmed temperature at a  
128 heating rate of 20°C/min.

129 From the first set of experiments the optimal experimental conditions were chosen:  
130 physical activation temperature of 600°C, chemical activation temperature of 1000°C  
131 and KOH as activated agent. At these experimental conditions the second series of  
132 experiments was performed (Table 3). It was decided to include also ZnCl<sub>2</sub> as activated

133 agent in order to take into account results from previous publications (Rawal et al.,  
134 2018; Tian et al., 2019).

135

136 **Table 2: Data for the activated carbon preparation in the first set of experiments.**

137

Physical activation (°C)	Chemical activation (°C)	Activating agent	Reference
600	1000	NaOH	A1
600	1000	KOH	A2
800	1000	NaOH	A3
800	1000	KOH	A4
1000	600	NaOH	A5
1000	600	KOH	A6
1000	800	NaOH	A7
1000	800	KOH	A8

138

139

140 **Table 3: Data for the activated carbon preparation in the second set of experiments.**

Activating agent	Activating agent/sludge ratio (mL/g)	Reference
KOH	0.3	B1
KOH	0.4	B2
KOH	0.5	B3
KOH	0.7	B4
ZnCl <sub>2</sub>	0.3	B5
ZnCl <sub>2</sub>	0.4	B6
ZnCl <sub>2</sub>	0.5	B7
ZnCl <sub>2</sub>	0.7	B8

141

142

143 2.3. Commercial activated carbon



144 In order to compare the effectiveness of the prepared AC, a commercial granular AC for  
145 gas adsorption was tested in this study. This AC is from VWR (reference number  
146 22631.293). Table 4 illustrates the main characteristics given by the supplier.

147 **Table 4: Technical characteristics of the commercial AC.**

Parameter	Values
Density (g/cm <sup>3</sup> )	2
Molecularweight (g/mol)	12.01
Meltingpoint (°C)	3550
Benzeneadsorption	38-42%

148

149

150

151 2.4. Characterization of prepared activated carbon

152

153 2.4.1. Specific surface area and isotherms analysis

154 The preparedactivated carbon wascharacterized in terms of surface area ( $S_{BET}$ ), total  
155 pore volume ( $V_t$ ) and average pore diameter ( $d_a$ ). BET method was applied using a  
156 Multi-port surface area and porosimetry analyser ASAP 2420 from Micromeritics  
157 (USA). Using this technology the micropore volume ( $V_m$ ) was also calculated. Total  
158 pore volume was calculated from the amount of adsorbed  $N_2$  at relative pressure ( $P/P_0$ )  
159 of 0.99 and average pore diameter was calculated following Eq. 1 as previously  
160 published in several studies (Pezoti et al. 2016; Zhang et al. 2019):

161

162 
$$d_a = \frac{4000 \cdot V_t}{S_{BET}} \quad (1)$$

163

164 In addition, adsorption isotherms were obtained using the prepared AC as shown in  
165 Table 2 and 3. Adsorption isotherms analysis is very important to study the interaction  
166 between the adsorbate and the adsorbent of a system (Cheng et al. 2018). In this study,  
167 BET isotherms were calculated. BET model assumes that adsorption process occurs in a  
168 multilayer of adsorbates with lateral interactions (Carrete et al. 2011).

169 The mathematical expression BET isotherm is described in Eq.2:

170

$$171 \frac{P}{V \cdot (P_0 - P)} = \frac{1}{V_m \cdot c} + \frac{c-1}{V_m \cdot c} \cdot \frac{P}{P_0} (2)$$

172 Where,  $P$  (mm Hg) and  $P_0$  (mm Hg) are the equilibrium and the saturation pressures,  
173 respectively, of adsorbates at the adsorption temperature,  $V$  (cm<sup>3</sup>/g) and  $V_m$  (cm<sup>3</sup>/g) are  
174 the adsorbed gas quantity and the monolayer adsorbed gas quantity, respectively and,  $c$   
175 is the BET constant.

176

#### 177 2.4.2. Microscopy analysis

178 The surface morphologies of the prepared AC were examined by observation of the  
179 microporous structure by means of a Field Emission Scanning Microscopy (FE-SEM)  
180 model Ultra 55 from Oxford Instruments (United Kingdom).

181

#### 182 2.4.3. Zeta potential

183 Zeta potential of the prepared AC was measured by Zetasizer Nano ZS90 (Malvern  
184 instruments, Malvern, United Kingdom). Zeta potential of the AC was measured by  
185 mixing the AC with distilled water at pH 7.5.

186

187

## 188 2.5. Activated carbon regeneration procedure

189 A regeneration process was carried out for the prepared activated carbon. The spent AC  
190 was placed in a laboratory beaker with 500 ml of NaOH at pH 10. This solution was  
191 stirred in a temperature controlled shaker at 200 rpm and 90°C during 2 hours. After this  
192 chemical regeneration process, the AC was filtered (with a paper filter of 60 µm) and  
193 rinsed with water until a neutral pH was reached. Afterwards, the AC was filtered again  
194 and was dried at 105°C during 12 hours.

195

## 196 2.6. Hydrogen sulphide adsorption equipment

197 Tests with laboratory columns were used for gas adsorption with the selected AC. Gas  
198 cylinders (provided by Abelló-Linde, Spain) containing a mixture of H<sub>2</sub>S/N<sub>2</sub> with a H<sub>2</sub>S  
199 concentration of 80 mg/L provided the feed to the adsorption column. These  
200 experiments were carried out in a glass column of 1.5 cm internal diameter and 20 cm  
201 length. A felt layer and a circular mesh were placed at the bottom of the column to  
202 ensure the correct package of the activated carbon. Fig. 1 shows the experimental set up  
203 used for the experiments.

204 Bed heights of the packed AC, mass of the AC and feed gas flow rate used in the tests  
205 are summarized in Table 5. The tests were stopped when the outlet and inlet H<sub>2</sub>S  
206 concentrations were approximately the same. It is important to mention that only the  
207 prepared ACs under the selected conditions were tested in the adsorption column.

208 In addition, in order to compare the saturation capacity of each AC tested, it was  
209 calculated the amount of H<sub>2</sub>S adsorbed per gram of AC used as it was expressed in Eq.  
210 3. This equation was previously applied also employed by Kuroda et al.(2018).

211

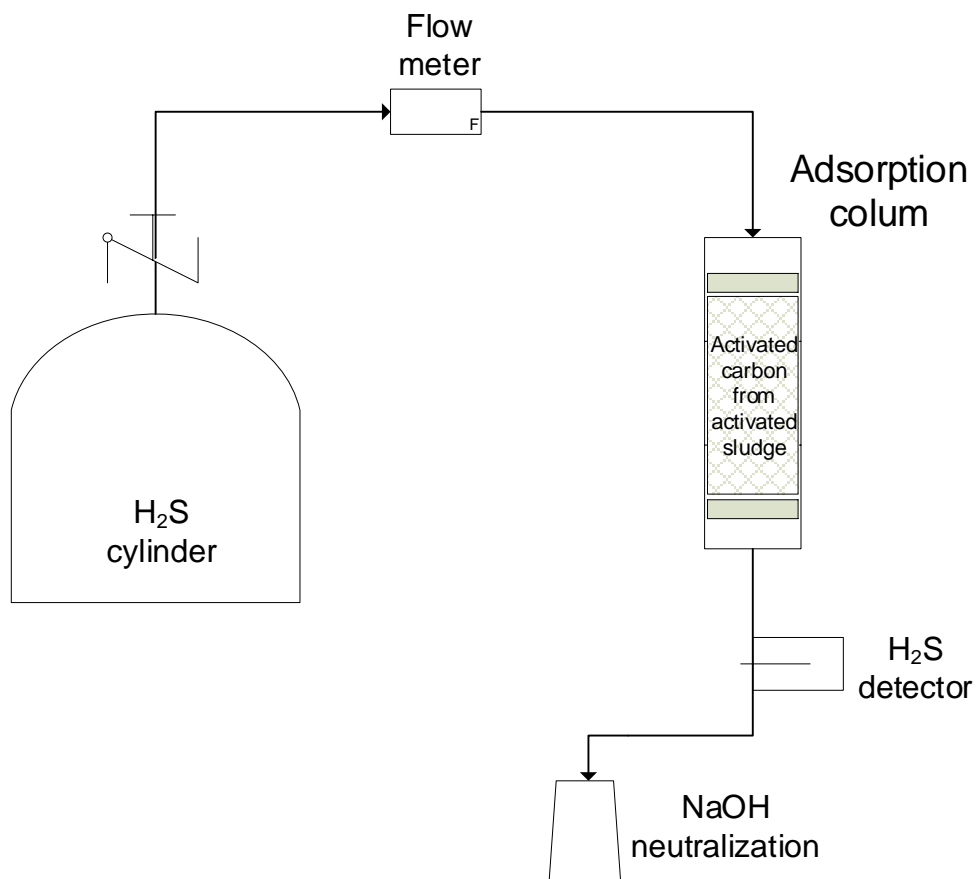
$$212 \text{ Capacity (mg H}_2\text{S adsorbed/g AC used)} = \frac{\left[ C_f \cdot t_f - \int_0^{t_f} C(t) dt \right] \cdot \frac{34g}{mol} \cdot Q}{m_{AC} \cdot 22,4 \text{ L/mol}} \quad (3)$$

213

214 Where, C<sub>f</sub> and t<sub>f</sub> are the final H<sub>2</sub>S concentration and time detected, respectively, Q is the  
215 flow rate employed and m<sub>AC</sub> is the AC mass used for each experiment.

216

217



218

219

**Figure 1: Experimental set up used for the adsorption column experiments.**

220

221

222

**Table 5: Experimental variables applied for the adsorption experiments.**

Test number	AC type	AC mass (g)	Bed heights (cm)	Flow rate (L/h)
1	Commercial AC	10.21	4	43
2	Prepared AC 1	2.09	2	43
3	Prepared AC 2	3.51	2	43
4	Regenerated AC 2	2.04	2	43

223

224

225

### 226 3. Results and discussion

227

228 3.1. Prepared activated carbon characteristics

229 3.1.1. Effect of temperature and activating agent

230 Pyrolysis temperature, carbonization time and impregnation ratio are the main  
231 parameters that can influence the surface area of the made ACs(Kacan, 2016). In order  
232 to study the effect of temperature, Table 6 illustrates the Brunauer-Emmet-Teller  
233 surface area ( $S_{BET}$ ), the total pore volume ( $V_t$ ), the micropore volume ( $V_m$ ) and the  
234 average pore diameter ( $d_a$ ) of the different samples of activated carbons that were  
235 obtained by means of the analysis of  $N_2$  adsorption. These results indicated that there  
236 was no direct influence of the physical activation temperature on the  $S_{BET}$ ,  $V_t$  and  $V_m$   
237 since the highest results were achieved for the lowest temperatures tested. The same  
238 conclusion was reported by Wang et al.(2018) who stated that a pyrolysis temperature  
239 of  $600^\circ$  was sufficient for sludge carbonization.However, it can be observed that when  
240 chemical activation temperature increased, the  $S_{BET}$ ,  $V_t$ and  $V_m$ increased. In addition, the  
241 best activating agent wasKOH,also in terms of  $S_{BET}$ ,  $V_t$  and  $V_m$ .Concerning the average  
242 pore diameter, all the values ranged between 2 and 20 nm, which means that no  
243 significant differences among the prepared ACs were found. The average pore diameter  
244 depends mainly on the reaction time, which was maintained constant in all the tests.  
245 Temperature also influences the pore size. However, the relation between temperature  
246 and pore size is complex. In this way,Satya Sai and Krishnaiah (2005) reported that at  
247  $800^\circ C$  low size pores are formed, but at  $850^\circ C$  the smaller pores become larger by  
248 coalescence phenomena. It explains that no relation between the experimental  
249 conditions and the average pore diameter was found.Taking into account these results,  
250 the best AC was the AC A2 since it was made with the highest  $S_{BET}$ ,  $V_t$  and  $V_m$ .

251 These results are in concordance with other studies found in the literature of AC  
252 preparation from sewage sludge. For example, Li et al. (2011) fabricated AC from sludge  
253 and achieved an AC with specific surface area between 130-140 m<sup>2</sup>/g. Wang et  
254 al. (2018) obtained an AC from sludge with a higher surface area (641.56 m<sup>2</sup>/g).

255 Regarding AC preparation from other raw materials, Li et al., (2019) reported that AC  
256 preparation from petroleum coke by KOH activation achieved S<sub>BET</sub> between 892-1,763  
257 m<sup>2</sup>/g and V<sub>t</sub> values between 0.39 and 0.48 cm<sup>3</sup>/g. Kazak et al. (2018) published that AC  
258 preparation from molasses-to-ethanol-process waste by KOH activation presented a  
259 S<sub>BET</sub> area of 1,042 m<sup>2</sup>/g and V<sub>t</sub> of 0.691 cm<sup>3</sup>/g. Sulaiman et al. (2018) fabricated AC  
260 from cassava stem and the carbon fabricated showed a maximum S<sub>BET</sub> area of 653.93  
261 m<sup>2</sup>/g. The difference between the previously published results and those reported in this  
262 study in terms of surface area was due to the raw material employed. Sewage sludge is  
263 not the best option to produce AC but results presented here demonstrated that it is a  
264 waste whose activation can produce an adsorbent with a S<sub>BET</sub> high enough to be  
265 competitive compared to other activated carbon materials (Chen et al. 2019).

266

### 267 3.1.2. Comparison of KOH and ZnCl<sub>2</sub> as activating agents

268 According to Tian et al. (2019), H<sub>3</sub>PO<sub>4</sub>, KOH, and ZnCl<sub>2</sub> are common activating agents  
269 in the AC preparation. In order to study the ZnCl<sub>2</sub> effect on the AC characteristics  
270 (Table 7), the experimental conditions from the first set of experiments (physical  
271 temperature of 600°C, chemical temperature of 1000°C and KOH as activated agent, AC  
272 type A2) study the effect of ZnCl<sub>2</sub> in comparison with KOH as activating agent. It can  
273 be observed in Table 7 that using KOH as activating agent (AC B1, B2, B3 and B4) led  
274 to higher S<sub>BET</sub> and V<sub>t</sub> than those obtained by using ZnCl<sub>2</sub> (AC B5, B6, B7 and B8). These

275 results are interesting since KOH is less expensive and less toxic than ZnCl<sub>2</sub> (Arami-Niya et al.  
276 2010; Donald et al. 2011). In addition, as it can be observed in Table 7, as activation  
277 agent/sludge ratio increased, S<sub>BET</sub> increased for both activating agents. These results are in  
278 the same range as those previously published by Sun et al. (2018), who prepared activated  
279 biochar from mixed waste plastic using ZnCl<sub>2</sub> as activating agent and obtained values of  
280 S<sub>BET</sub> between 661 and 1032 m<sup>2</sup>/g, V<sub>t</sub> values between 0.44 and 0.64 cm<sup>3</sup>/g and d<sub>a</sub> values  
281 between 2.15 and 3.62 nm.



282

283

Table 6: Surface area ( $S_{BET}$ ), total pore volume ( $V_t$ ), micropore volume ( $V_m$ ) and average pore diameter ( $d_a$ ) of the first set of experiments.

Activated carbon type	A1	A2	A3	A4	A5	A6	A7	A8
$S_{BET}$ ( $m^2/g$ )	$140.29 \pm 7.01$	$375.13 \pm 18.75$	$185.95 \pm 9.29$	$236.4 \pm 11.82$	$143.3 \pm 7.17$	$1.57 \pm 0.08$	$55.57 \pm 2.78$	$187.34 \pm 9.37$
$V_m$ ( $cm^3/g$ )	$0.0488 \pm 0.05$	$0.1587 \pm 0$	$0.0617 \pm 0$	$0.1031 \pm 0.01$	$0.0468 \pm 0$	$0.002 \pm 0$	$0.012 \pm 0$	$0.0595 \pm 0$
$V_t$ ( $cm^3/g$ )	$0.1765 \pm 0.17$	$0.3152 \pm 0.01$	$0.2321 \pm 0.01$	$0.1465 \pm 0.01$	$0.1148 \pm 0$	$0.0072 \pm 0$	$0.1594 \pm 0.01$	$0.1917 \pm 0.01$
$d_a$ (nm)	$5.03 \pm 5.03$	$3.36 \pm 0.17$	$4.99 \pm 0.25$	$2.48 \pm 0.12$	$3.2 \pm 0.16$	$18.32 \pm 0.91$	$11.48 \pm 0.57$	$4.09 \pm 0.20$

284

285

286

Table 7: Surface area ( $S_{BET}$ ), total pore volume ( $V_t$ ), micropore volume ( $V_m$ ) and average pore diameter ( $d_a$ ) of the second set of experiments.

Activated carbon type	B1	B2	B3	B4	B5	B6	B7	B8
Activated agent	KOH	KOH	KOH	KOH	ZnCl <sub>2</sub>	ZnCl <sub>2</sub>	ZnCl <sub>2</sub>	ZnCl <sub>2</sub>
$S_{BET}$ ( $m^2/g$ )	$287.99 \pm 14.40$	$338.54 \pm 16.93$	$342.78 \pm 17.14$	$340.18 \pm 17.01$	$184.42 \pm 9.22$	$204.95 \pm 10.24$	$228.25 \pm 11.41$	$228.59 \pm 11.42$
$V_m$ ( $cm^3/g$ )	$0.1138 \pm 0.01$	$0.1374 \pm 0.01$	$0.1307 \pm 0.01$	$0.1117 \pm 0.01$	$0.0524 \pm 0$	$0.0621 \pm 0$	$0.0702 \pm 0$	$0.0698 \pm 0$
$V_t$ ( $cm^3/g$ )	$0.2051 \pm 0.01$	$0.2190 \pm 0.01$	$0.2471 \pm 0.01$	$0.2850 \pm 0.01$	$0.1757 \pm 0.01$	$0.1828 \pm 0.01$	$0.2065 \pm 0.01$	$0.2135 \pm 0.01$
$d_a$ (nm)	$2.85 \pm 0.14$	$2.59 \pm 0.13$	$2.88 \pm 0.14$	$3.35 \pm 0.17$	$3.81 \pm 0.19$	$3.57 \pm 0.18$	$3.62 \pm 0.18$	$3.74 \pm 0.19$

287

288

### 289 3.1.3. Isotherm analysis

290 According to the International Union of Pure and Applied Chemistry (IUPAC) standard  
291 classification system, there are six different types of adsorptionSing et al.(1985) as it  
292 can be observed in a previous publication (Wei Yu, 2018). In this way, depending of the  
293 shape of the adsorption isotherm, the properties of the adsorbate and solid adsorbent and  
294 the pore-space geometry can be different. Detailed information about it can be found in  
295 (Sing et al.1985). Fig. 2 represents BET isotherms of prepared AC in the testsA2 and  
296 B3. It can be observed that both curves showed a convex curvature at low relative  
297 pressures ( $P/P_0$  lower than 0.2) and then a slight hysteresis towards  
298 saturation.Adsorption normally occurs in a nonporous or a macroporouslayer(Singet  
299 al.1985). In this way, adsorption process seems to be in the multi-layer coverage since  
300 there is a clear inflection in the isotherm (Lapham and Lapham, 2017a).

301 Table 8 shows the BET c-value for all the AC fabricated. According to Ladavos et  
302 al.(2012), who investigated the BET isotherm model in porous materials for gas  
303 adsorption, c-values should be greater than zero.Lapham and Lapham (2017b) published  
304 that BET c-values higher than 20 confirms that  $S_{BET}$  and adsorption isotherms  
305 previously calculated are reliable and valid. As it can be observed in Table 8, c-values  
306 were always positive and higher than 20.

307

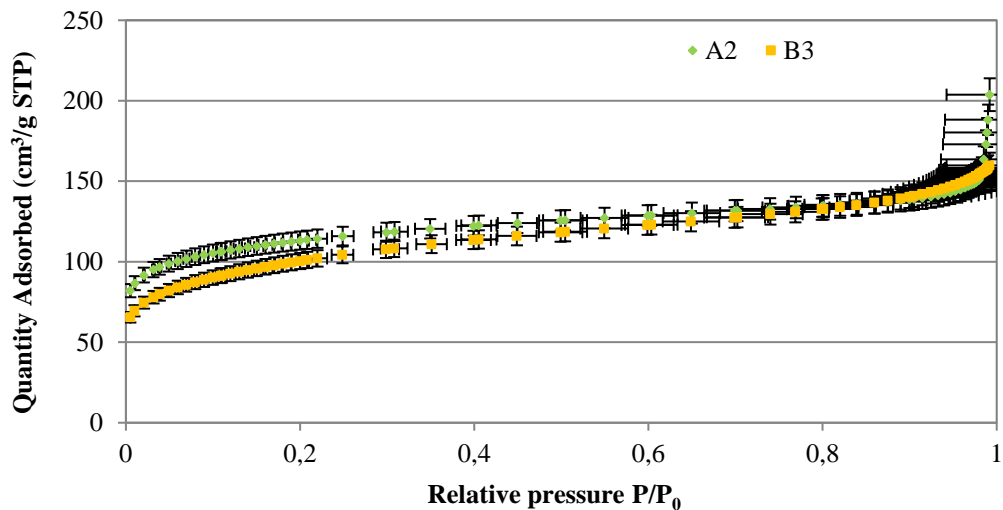


Figure 2: BET isotherm for AC A2 and B3.

Table 8: BET c-value for each prepared AC.

<b>AC first set of experiments</b>	<b>A1</b>	<b>A2</b>	<b>A3</b>	<b>A4</b>	<b>A5</b>	<b>A6</b>	<b>A7</b>	<b>A8</b>
<b>BET c-value</b>	335.44	302.08	291.86	179.92	339.55	29.84	1092.56	465.06
<b>AC second set of experiments</b>	<b>B1</b>	<b>B2</b>	<b>B3</b>	<b>B4</b>	<b>B5</b>	<b>B6</b>	<b>B7</b>	<b>B8</b>
<b>BET c-value</b>	243.88	467.17	241.78	233.18	431.71	442.36	300.84	364.46

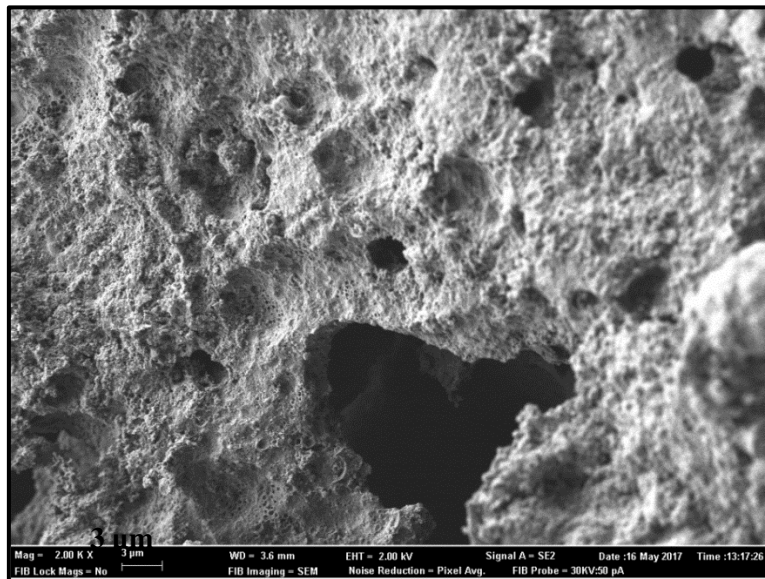
#### 3.1.4. Microscopy results

The surfaces morphologies of the prepared AC with the highest areas (A2 and B3 for the first and second series of experiments, respectively) are shown in Fig. 3. Both AC had a very similar surface area (375 and 342 m<sup>2</sup>/g for AC of A2 and B3, respectively) which is in agreement with these FE-SEM pictures since a very similar structure can be observed in Fig. 3. FE-SEM images show a highly porous structure, a relatively uniform surface and without the crevices appearance. The surface seems to be heterogeneous and with a variety of randomly distributed micropores and nanopores of different sizes

323 (diameter around 0.1  $\mu\text{m}$ ). The different pore sizes can be attributed to the organic  
324 matter decomposition during the carbonization process. In addition, the size and the  
325 presence of particles is reduced due to material loss during pyrolysis process.

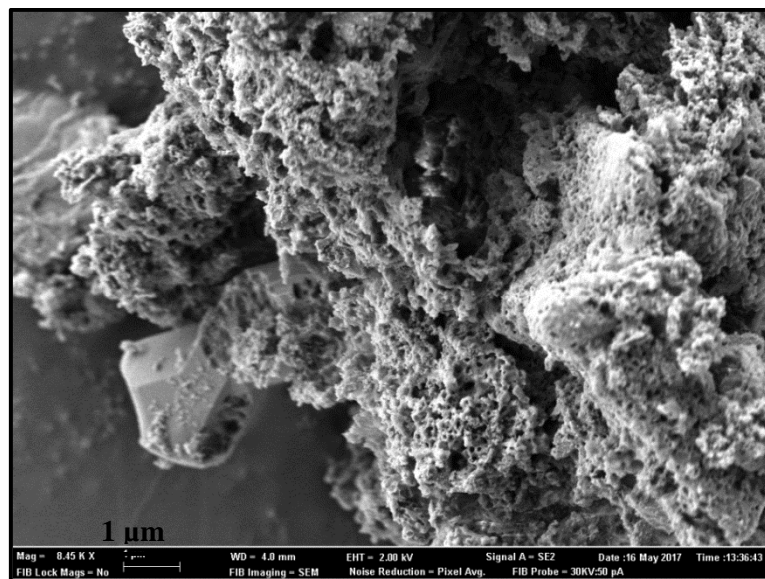
326

327 a)



329

330 b)



332

Figure 3: FE-SEM images of the prepared AC samples number a)A2 and b) B3.

### 333 3.1.5. Zeta potential results

334 Zeta potential of the tested AC for H<sub>2</sub>S adsorption (AC1 and AC2) was measured to  
335 study possible interactions between the AC and the H<sub>2</sub>S during the adsorption process.  
336 The mean value of zeta potential of AC1 and AC2 was  $-24.9 \pm 0.8$  mV and  $-25.2 \pm 1$  mV,  
337 respectively. Thus, both values were very similar. They clearly showed the negative  
338 charge of the prepared AC. This fact suggests that positively charged pollutants will be  
339 more easily adsorbed by these AC. For H<sub>2</sub>S adsorption, the presence of H<sup>+</sup> protons  
340 forming a dipole moment with S<sup>-2</sup> can result favourable for the H<sub>2</sub>S adsorption. This fact  
341 is due to the negative charge of the prepared AC and the positive electric density of the  
342 H<sup>+</sup>. In addition, this result is in concordance with Li et al. (2011) who also published a  
343 negative zeta potential value of sludge-based AC (between -35 and -37 mV).

344

### 345 3.2. Hydrogen sulphide adsorption

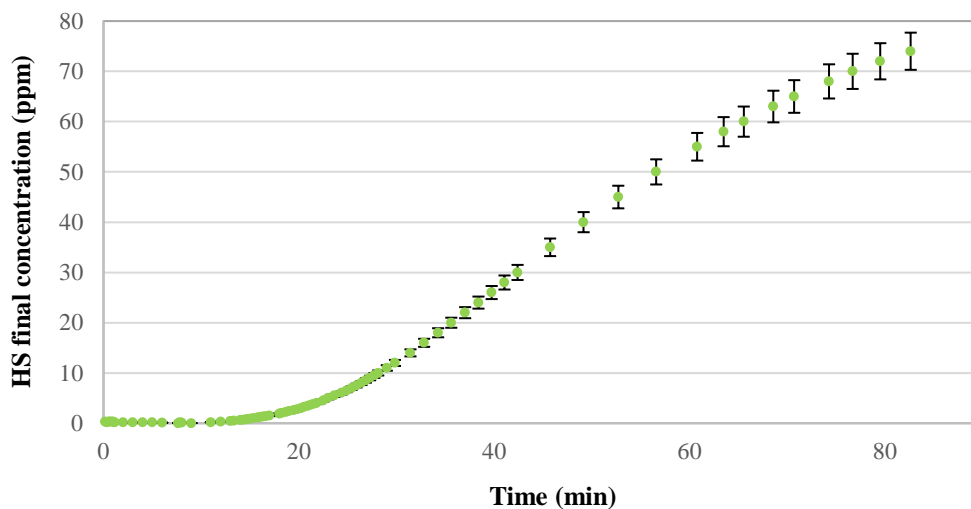
346 In order to study the effectiveness in the H<sub>2</sub>S removal of the prepared AC, regenerated  
347 AC and a commercial AC, breakthrough curves have been plotted (Fig. 4). H<sub>2</sub>S retention  
348 capacity was measured using an H<sub>2</sub>S initial concentration of 80 ppm in the feed gas. It  
349 can be observed that the breakpoint occurred at approximately 30 min for commercial  
350 AC whereas for the AC 1, AC 2 and regenerated AC 2, it occurred at about 140, 90 and  
351 7 min, respectively. It can be observed that the prepared ACs showed higher affinity to  
352 H<sub>2</sub>S retention than the commercial AC since the breakpoints occurred later than in the  
353 case of the commercial AC. As expected, since no thermal treatment was performed, the  
354 regenerated AC 2 did not show the same efficiency than the new AC 2. These results  
355 are in concordance with previous studies such as Zhang et al. (2016) who prepared AC  
356 from black liquor for hydrogen sulphide removal and reported that the breakpoint was

357 around 150 minutes. Regarding H<sub>2</sub>S adsorption mechanism on activated carbon,  
358 according Shen et al.(2018) AC can facilitate the H<sub>2</sub>S molecule dissociation and offers  
359 active sites for H<sub>2</sub>S adsorption.

360 In order to compare the saturation capacity of each AC, Table 9 shows the relation  
361 between the H<sub>2</sub>S adsorbed mass (in mg) and the AC mass (in g) employed in each test.  
362 It can be observed, as commented above, that the commercial AC had a lower capacity  
363 than the prepared AC, even than the regenerated AC. De Falco et al.(2018) tested a  
364 commercial AC impregnated with Cu and Zn for H<sub>2</sub>S removal and achieved a  
365 adsorption capacity values between 6.8 and 49.64 mg/g. However, Aslam et al.(2015)  
366 prepared AC from oil fly ash for H<sub>2</sub>S removal from a gas stream and obtained saturation  
367 capacity values around 0.1 mg/g. Taking into account these results, it can be concluded  
368 that the results published here are in the range with previous results published in the  
369 bibliography.

370

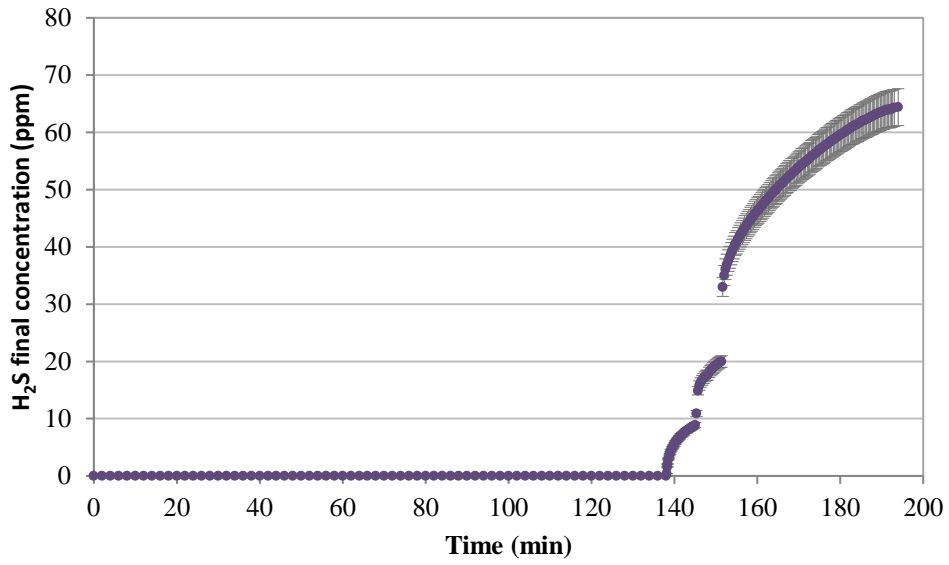
371 a)



372

373

374 b)

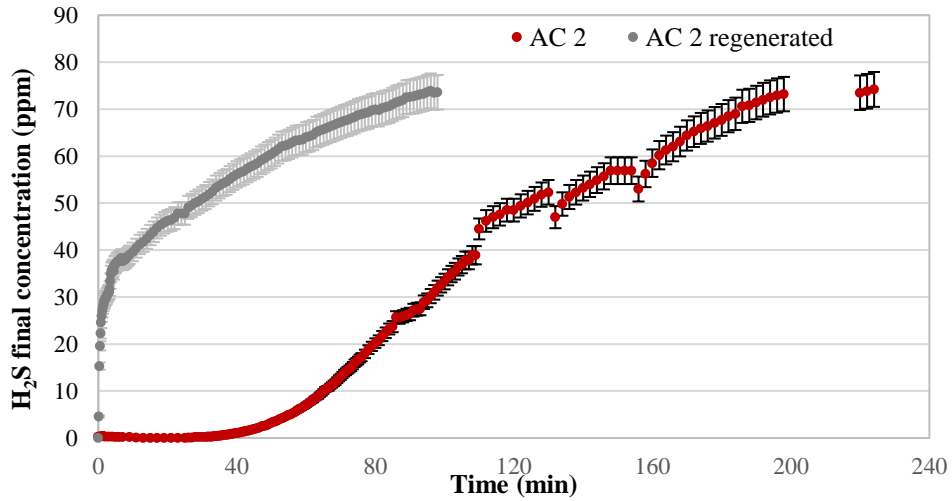


375

376

377

378 c)



379

380

381

382

383

384

Figure 4: Experimental and breakthrough curves for a) commercial AC, b) AC 1 and c) AC 2.

385

**Table 9: Capacity of each AC.**

AC type	Commercial AC	AC 1	AC 2	Regenerated AC 2
adsorbed H <sub>2</sub> S (mg)/AC mass (g)	0.37	5.0	1.96	0.78

386

387

#### 388 **4. Conclusions**

389

390 In this study, AC with interesting properties for hydrogen sulphide removal was  
 391 prepared from sewage sludge by physical-chemical activation. The optimum physical  
 392 and chemical activation temperature was 600°C and 1000°C, respectively. Regarding  
 393 the best activated agent, KOH achieved the most interesting results in terms of specific  
 394 surface area (values around 300 and 340 m<sup>2</sup>/g for the tested conditions). Zeta potential of  
 395 the prepared AC was negative (around -25 mV) and it was observed a heterogeneous  
 396 pore size distribution in the surface morphology of the adsorbent materials. In addition,  
 397 the experimental results were adjusted to BET isotherms, which confirms that the  
 398 adsorption process occurs in a multi-layer space. Finally, results from the prepared and  
 399 the commercial AC tested for H<sub>2</sub>S removal demonstrated that the prepared AC was  
 400 effective, even more than the tested commercial AC, for H<sub>2</sub>S removal. As a general  
 401 conclusion, it can be confirmed that the use of prepared AC from sewage sludge for  
 402 odours removal could be of great interest in a recent future.

#### 403 **References**

404 Andrade, S.N., Veloso, C.M., Fontan R.C.I, Bonomo, R.C.F., Santos, L.S., Brito, M.J.P.,  
 405 Diniz, G.A.(2018). Chemical-activated carbon from coconut (cocos nucifera) endocarp  
 406 waste and its application in the adsorption of beta lactoglobulin protein. Rev. Mex. Ing.  
 407 Química 17 (2), 463–475.



408 APHA, AWWA, WEF, Standard Methods for the Examination of Water and  
409 Wastewater., 2005. Washington.

410 Arami-Niya, A., Daud, W.M.A.W., Mjalli, F.S., (2010). Using granular activated  
411 carbon prepared from oil palm shell by ZnCl<sub>2</sub> and physical activation for methane  
412 adsorption. *J. Anal. Appl. Pyrolysis* 89, 197–203.

413 Aslam, Z., Shawabkeh, R., Hussein, I., Al-Baghli, N., Eic, M., (2015). Synthesis of  
414 activated carbon from oil fly ash for removal of H<sub>2</sub>S from gas stream. *Appl. Surf. Sci.*  
415 327, 107–115.

416 Carrete, J., García, M., Rodríguez, J.R., Cabeza, O., Varela, L.M., (2011). Fluid Phase  
417 Equilibria Theoretical model for moisture adsorption on ionic liquids: A modified  
418 Brunauer – Emmet – Teller isotherm approach. *Fluid Phase Equilib.* 301, 118–122.

419 Chen, C.L., Park, S.W., Su, J.F., Yu, Y.H., Heo, J. eun, Kim, K. duk, Huang,  
420 C.P.(2019). The adsorption characteristics of fluoride on commercial activated carbon  
421 treated with quaternary ammonium salts (Quats). *Sci. Total Environ.* 693, 133605.

422 Cheng, S., Zhang, L., Ma, A., Xia, H., Peng, J., Li, C., Shu, J.(2018). Comparison of  
423 activated carbon and iron/cerium modified activated carbon to remove methylene blue  
424 from wastewater. *J. Environ. Sci.* 65, 92–102.

425 Chiavola, A., (2013). Textiles. *Water Environ. Res.* 85, 1581–1600.

426 De Falco, G., Montagnaro, F., Balsamo, M., Erto, A., Deorsola, F.A., Lisi, L., Cimino,  
427 S.(2018). Synergic effect of Zn and Cu oxides dispersed on activated carbon during  
428 reactive adsorption of H<sub>2</sub>S at room temperature. *Microporous Mesoporous Mater.* 257,  
429 135–146.

430 Donald, J., Ohtsuka, Y., Xu, C.C. (2011). Effects of activation agents and intrinsic  
431 minerals on pore development in activated carbons derived from a Canadian peat.  
432 *Mater. Lett.* 65, 744–747.

433 F. Li, T. Lei, Y. Zhang, J. Wei, Y.Y.(2015). Preparation, characterization of sludge  
434 adsorbent and investigations on its removal of hydrogen sulfide under room  
435 temperature. *Front. Environ. Sci. Eng.* 9 (2), 190–196.

436 G. Mininni, A.R. Blanch, F. Lucena, S.B.(2015). EU policy on sewage sludge  
437 utilization and perspectives on new approaches of sludge management. *Environ. Sci.*  
438 *Pollut. Res.* 22, 7361–7374.

439 G.S. dos Reis, M.K. B. Mahbub, M. Wilhelm, E. C. Lima, C. H. Sampaio, C. Saucier,  
440 S.L.P.D.(2016). Activated carbon from sewage sludge for removal of sodium diclofenac  
441 and nimesulide from aqueous solutions. *Korean J. Chem. Engineering* 33 (11), 3149–  
442 3161.

443 J. M. Dias, M.C.M. Alvim-Ferraz, M. F. Almeida, J. Rivera-Utrilla, M.S.-P.(2007).  
444 Waste materials for activated carbon preparation and its use in aqueous-phase treatment:  
445 A review. *J. Environ. Manage.* 85, 833–846.

446 J. Zhu, Y.H. Li, L. Xu, Z.Y.L.(2018). Removal of toluene from waste gas by  
447 adsorption-desorption process using corncob-based activated carbons as adsorbents.  
448 *Ecotoxicol. Environ. Saf.* 165, 115–125.

449 Kacan, E.(2016). Optimum BET surface areas for activated carbon produced from  
450 textile sewage sludges and its application as dye removal. *J. Environ. Manage.* 166,  
451 116–123.

452 Kazak, O., Eker, Y.R., Bingol, H., Tor, A.(2018). Preparation of chemically-activated  
453 high surface area carbon from waste vinasse and its efficiency as adsorbent material. *J.*  
454 *Mol. Liq.* 272, 189–197.

455 Kimura, K., Honoki, D., Sato, T.(2017). Effective physical cleaning and adequate  
456 membrane flux for direct membrane filtration (DMF) of municipal wastewater: Up-  
457 concentration of organic matter for efficient energy recovery. *Sep. Purif. Technol.* 181,

458 37–43.

459 Kuroda, S., Nagaishi, T., Kameyama, M., Koido, K., Seo, Y., Dowaki, K.(2018).  
460 Hydroxyl aluminium silicate clay for biohydrogen purification by pressure swing  
461 adsorption: Physical properties, adsorption isotherm, multicomponent breakthrough  
462 curve modelling, and cycle simulation. *Int. J. Hydrogen Energy* 43, 16573–16588.

463 Ladavos, A.K., Katsoulidis, A.P., Iosifidis, A., Triantafyllidis, K.S., Pinnavaia, T.J.,  
464 Pomonis, P.J.(2012). Microporous and Mesoporous Materials The BET equation , the  
465 inflection points of N<sub>2</sub> adsorption isotherms and the estimation of specific surface area  
466 of porous solids. *Microporous Mesoporous Mater.* 151, 126–133.

467 Lapham, D.P., Lapham, J.L.(2017a). Gas adsorption on commercial magnesium  
468 stearate : Effects of degassing conditions on nitrogen BET surface area and isotherm  
469 characteristics. *Int. J. Pharm.* 530, 364–376.

470 Lapham, D.P., Lapham, J.L.(2017b). Gas adsorption on commercial magnesium  
471 stearate : Effects of degassing conditions on nitrogen BET surface area and isotherm  
472 characteristics. *Int. J. Pharm.* 530, 364–376.

473 Li, D., Zhou, J., Wang, Y., Tian, Y., Wei, L., Zhang, Z., Qiao, Y., Li, J.(2019). Effects  
474 of activation temperature on densities and volumetric CO<sub>2</sub> adsorption performance of  
475 alkali-activated carbons. *Fuel* 238, 232–239.

476 Li, J., Xing, X., Li, J., Shi, M., Lin, A., Xu, C., Zheng, J., Li, R.(2018). Preparation of  
477 thiol-functionalized activated carbon from sewage sludge with coal blending for heavy  
478 metal removal from contaminated water. *Environ. Pollut.* 234, 677–683.

479 Li, W.H., Yue, Q.Y., Gao, B.Y., Ma, Z.H., Li, Y.J., Zhao, H.X. (2011). Preparation and  
480 utilization of sludge-based activated carbon for the adsorption of dyes from aqueous  
481 solutions. *Chem. Eng. J.* 171, 320–327.

482 Li, Y. Huan, Chang, F. Min, Huang, B., Song, Y. Peng, Zhao, H. Yu, Wang, K. Jun,

483 (2020). Activated carbon preparation from pyrolysis char of sewage sludge and its  
484 adsorption performance for organic compounds in sewage. *Fuel* 266, 117053.

485 M. Qiu, C.H. (2015). Removal of dyes from aqueous solution by activated carbon from  
486 sewage sludge of the municipal wastewater treatment plant. *Desalin. Water Treat.* 53,  
487 3641–3648.

488 P. Hadi, M. Xu, C. Ning, C.S.K. Lin, G.M.(2015). A critical review on preparation,  
489 characterization and utilization of sludge-derived activated carbons for wastewater  
490 treatment. *Chem. Eng. J.* 260, 895–906.

491 Pandiarajan, A., Kamaraj, R., Vasudevan, S., Vasudevan, S.(2018). OPAC (orange peel  
492 activated carbon) derived from waste orange peel for the adsorption of  
493 chlorophenoxyacetic acid herbicides from water: Adsorption isotherm, kinetic  
494 modelling and thermodynamic studies. *Bioresour. Technol.* 261, 329–341.

495 Peng, L., Dai, H., Wu, Y., Peng, Y., Lu, X.(2018). A Comprehensive Review of the  
496 Available Media and Approaches for Phosphorus Recovery from Wastewater. *Water.*  
497 *Air. Soil Pollut.* 229.

498 Pezoti, O., Cazetta, A.L., Bedin, K.C., Souza, L.S., Martins, A.C., Silva, T.L., Santos  
499 Júnior, O.O., Visentainer, J. V., Almeida, V.C.(2016). NaOH-activated carbon of high  
500 surface area produced from guava seeds as a high-efficiency adsorbent for amoxicillin  
501 removal: Kinetic, isotherm and thermodynamic studies. *Chem. Eng. J.* 288, 778–788.

502 Ping, Q., Zheng, M., Dai, X., Li, Y.(2020). Metagenomic characterization of the  
503 enhanced performance of anaerobic fermentation of waste activated sludge with CaO<sub>2</sub>  
504 addition at ambient temperature: Fatty acid biosynthesis metabolic pathway and  
505 CAZymes. *Water Res.* 170, 115309.

506 Rawal, S., Joshi, B., Kumar, Y.(2018). Synthesis and characterization of activated  
507 carbon from the biomass of *Saccharum bengalense* for electrochemical supercapacitors.

508 J. Energy Storage 20, 418–426.

509 Satya Sai, P.M., Krishnaiah, K.(2005). Development of the pore-size distribution in  
510 activated carbon produced from coconut shell char in a fluidized-bed reactor. Ind. Eng.  
511 Chem. Res. 44, 51–60.

512 Shen, F., Liu, J., Zhang, Z., Dong, Y., Gu, C.(2018). Density functional study of  
513 hydrogen sulfide adsorption mechanism on activated carbon. Fuel Process. Technol.  
514 171, 258–264.

515 Sing, K.S.W., Everett, D.H., Haul, R.A.W., Moscou, L., Pierotti, R.A., Rouquerol, J.,  
516 Siemieniewska, T.(1985). Reporting physisorption data for gas/solid systems with  
517 special reference to the determination of surface area and porosity. Pure Appl. Chem.  
518 57.

519 Sulaiman, N.S., Hashim, R., Mohamad Amini, M.H., Danish, M., Sulaiman, O. (2018).  
520 Optimization of activated carbon preparation from cassava stem using response surface  
521 methodology on surface area and yield. J. Clean. Prod. 198, 1422–1430.

522 Sun, K., Huang, Q., Chi, Y., Yan, J.(2018). Effect of ZnCl<sub>2</sub>-activated biochar on  
523 catalytic pyrolysis of mixed waste plastics for producing aromatic-enriched oil. Waste  
524 Manag. 81, 128–137.

525 Tian, D., Xu, Z., Zhang, D., Chen, W., Cai, J., Deng, H., Sun, Z., Zhou, Y.(2019).  
526 Micro–mesoporous carbon from cotton waste activated by FeCl<sub>3</sub>/ZnCl<sub>2</sub>: Preparation,  
527 optimization, characterization and adsorption of methylene blue and eriochrome black  
528 T. J. Solid State Chem. 269, 580–587.

529 Wang, N., Zhang, W., Cao, B., Yang, P., Cui, F., Wang, D. (2018). Advanced anaerobic  
530 digested sludge dewaterability enhancement using sludge based activated carbon  
531 (SBAC) in combination with organic polymers. Chem. Eng. J. 350, 660–672.

532 Wang, X., Zhu, N., Yin, B.(2008). Preparation of sludge-based activated carbon and its

533 application in dye wastewater treatment. *J. Hazard. Mater.* 153, 22–27.

534 Wei Yu, K.S.(2018). Modeling Gas Adsorption in Marcellus Shale Using Langmuir and  
535 BET Isotherms, in: *Shale Gas and Tight Oil Reservoir Simulation*. pp. 129–154.

536 Ye, Y., Ngo, H.H., Guo, W., Liu, Y., Chang, S.W., Nguyen, D.D., Liang, H., Wang, J.  
537 (2018). A critical review on ammonium recovery from wastewater for sustainable  
538 wastewater management. *Bioresour. Technol.* 268, 749–758.

539 Zhang, J. ping, Sun, Y., Woo, M.W., Zhang, L., Xu, K.Z.(2016). Preparation of steam  
540 activated carbon from black liquor by flue gas precipitation and its performance in  
541 hydrogen sulfide removal: Experimental and simulation works. *Rev. Mex. Urol.* 76,  
542 395–404.

543 Zhang, Y., Song, X., Xu, Y., Shen, H., Kong, X. (2019). Utilization of wheat bran for  
544 producing activated carbon with high specific surface area via NaOH activation using  
545 industrial furnace. *J. Clean. Prod.* 210, 366–375.

546